Room temperature synthesis of spherical mesoporous titania

Aihua Sun [a,*], Zhixiang Li [b], Ming Li [a], Gaojie Xu [a], Yong Li [a], Ping Cui [a]

[a] Department of Functional Materials and Nano-Devices, Ningbo Institute of Materials Technology and Engineering, Chinese Academy of Sciences, Ningbo 315201, China
[b] Key Laboratory of Materials Physics, Institute of Solid State Physics, Chinese Academy of Sciences, Hefei 230031, China

ARTICLE INFO

ABSTRACT

This work reports a facile hydrolysis method for the synthesis of spherical mesoporous titania particles using titanium tetrachloride under mild conditions. The method can be easily controlled or expanded. The influences of various reaction conditions including concentration of Ti^{4+} ions and water content on the formation of mesoporous titania particles were systematically investigated. The titania particles were characterized by X-ray diffraction (XRD), field emission scanning electron microscope (FESEM), high-resolution transmission electron microscopy (HRTEM) and Brunauer–Emmett–Teller (BET) surface areas. Experimental results showed that the mesoporous titania particles have special surface structure and excellent thermally stable mesoporous structure after annealing at high temperatures (500 °C). The effects of various reaction conditions, such as concentration of Ti^{4+}, H_2O/n-butanol volume ratio and reaction temperature, on formation, crystal phase, morphology of titania particles were investigated.

Crown Copyright © 2010 Published by Elsevier B.V. All rights reserved.

1. Introduction

Mesoporous materials have attracted considerable interest mainly because of their high specific surface area, high damping capacity, low thermal conductivity, and low dielectric permittivity [1,2]. Many oxide porous materials have been prepared in the past several years, including TiO_2 [3–6], SiO_2 [7] and SnO_2 [8], etc. Among them, mesoporous TiO_2 and TiO_2-derived [9–11] materials have attracted much attention due to their high specific surface area and more active sites, which are of great importance in photocatalysis and photo-electrical chemical conversion. In the past decade, considerable efforts have been devoted to develop titania nanomaterials with well-structured, porous and high surface area. Antonelli and Ying [12] have reported the preparation of mesoporous titania through a sol–gel process in presence of phosphate. However these precipitates were not pure titania because a significant amount of phosphorous still remained. A phosphorus-free mesoporous titania prepared by a modified ligand-assisted templating method with amine surfactants was also reported by Antonelli [13]. However, the porous structure has not been retained after the treatment at 300 °C. In most cases, crystalline titania particles are required for their applications. Calcination of the as-prepared mesoporous TiO_2 at high temperature is essential for the crystallization of titania. As a result, severe damage to the mesoporous structure may take place. So, it is necessary to synthesis mesoporous TiO_2 with a crystalline framework via a low-

temperature process. Yue and Gao [14] have presented the first example of mesoporous TiO_2 with crystalline framework prepared through a hydrothermal process. Yang et al. [15] also reported mesoporous anatase TiO_2 powders prepared by urea thermal hydrolysis with PEG as a dispersant. Cabrera et al. [16] synthesized the thermally stable mesoporous pure TiO_2 by a self-assembling process. Khalil et al. [17] prepared mesoporous spherical titania particles via hydrolysis of pure titanium tetra-isopropoxide in n-heptane solution. Wang et al. [18] obtained mesoporous crystalline titania powders of 100–300 nm by a novel microwave hydrothermal process utilizing micelle in the sol–gel solution. However, these processes need special apparatus (such as stainless steel autoclave) or expensive raw materials (such as titanium tetra alkoxides). Preparation of mesoporous crystalline TiO_2 by thermal hydrolysis of the inexpensive titanyl sulphate and titanium chloride has been reported recently [19–22]. Chen et al. [19] prepared thermally stable mesoporous TiO_2 nanoparticles by amine surfactant-mediated templating method using $Ti(SO_4)_2$ solution. The specific surface areas of the mesoporous nanosized TiO_2 calcined at 400 and 500 °C were 189 and 151 m^2/g, respectively. So, the formation of crystalline mesoporous TiO_2 at lower temperature with inexpensive raw materials (such as TiCl4 or Ti (SO4)2) and simple process is important either on the study and application.

In this paper, a simple method to synthesize mesoporous titania nanoparticles is established. The synthesis of mesoporous titania has been carried out under mild hydrolysis condition from the mixed system titanium tetrachloride, n-butanol and water. At the same time, the process is easy to control and expand. The particle characteristics (e.g., shape, size, crystallization) of the as-prepared nanoparticles are

investigated by various advanced techniques. The influence of a few experimental parameters (e.g., the ratio of H_2O/n-butanol and concentration of Ti^{4+}) on the particle growth in the mixed solution is then investigated.

2. Experimental procedures

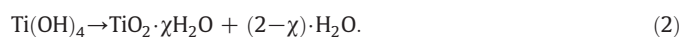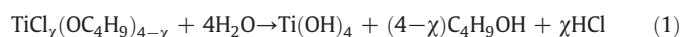### 2.1. Synthesis of mesoporous titania

The mesoporous titania nanoparticles could be prepared by the hydrolysis of $TiCl_4$ in a mixed solvent of n-butanol and water under mild conditions. This approach is similar to the previous studies [23], but the modification of experimental materials and parameters has been adopted to prepare spherical mesoporous titania nanoparticles. In a typical procedure, three steps were involved. First, 4 g $TiCl_4$ (Sinopharm Chemical Reagent Co., Ltd., China, CP, 98%) was put into 75 ml of n-butanol (Sinopharm Chemical Reagent Co., Ltd., China, AR, 99%) in an ice-water bath under vigorous stirring. Second, the transparent yellow solution was dripped into a three necked flask containing 25 ml of hot water (~80 °C) and 2 ml of triethanolamine (Sinopharm Chemical Reagent Co., Ltd., China, AR, 99%), followed by vigorous stirring to ensure that the reaction system was homogeneous. Finally, the mixed solution was refluxed heating at 80 °C for around 3 h, the white precipitate was centrifuged, washed with de-ionized water for five times and then dried in a vacuum oven at 80 °C. Ultra-pure water was used in all the synthesis processes.

2.2. Characterization

Particle characteristics such as shape and size were checked under field emission scanning electron microscopy (FESEM, Sirion 200 FEG) and transmission electron microscopy (TEM, JEM-2010), operated at an accelerated voltage of 5 kV and 200 kV, respectively. The specimens for FESEM observation were prepared by dispersing ultrasonically in de-ionized water and then placing on silicon substrate. The specimens for TEM observation prepared by dropping the solution onto a Formvar-coated copper grid and dried in air naturally. FT-IR spectra were recorded via KBr disks method on a Nicolet Magna-750 spectrometer. The powders are mixed with anhydrous KBr and squeezed under pressure to form disks, respectively. The as-prepared and calcined titania samples were characterized by using X-ray diffraction, the XRD patterns were recorded on a Philips X'pert PRO X-ray diffractometer with a 2θ ranging from 20 to 80 °, using Cu–Ka radiation ($\lambda = 0.1541$ nm). Brunauer–Emmett–Teller (BET) and Barrett–Joyner–Halenda (BJH) methods were used to determine the specific surface areas and pore sizes of the samples using a model ASAP 2010 Micrometrics Instrument, and the samples were degassed at 150 °C for 3 h to ensure that no gas molecules adsorbed on the particle surfaces. The size distribution of particle was measured by dynamic light scattering (DLS), using Malvern/Zeta sizer Nano ZS instrument.

3. Results and discussion

Spherical mesoporous titania are obtained through hydrolysis of titanium tetrachloride in a mixed solution of n-butanol and water at mild conditions. Hydrolysis and condensation take place in the simple process. The reactions (1) and (2) were shown in below:

$$TiCl_\chi(OC_4H_9)_{4-\chi} + 4H_2O \rightarrow Ti(OH)_4 + (4-\chi)C_4H_9OH + \chi HCl \qquad (1)$$

$$Ti(OH)_4 \rightarrow TiO_2 \cdot \chi H_2O + (2-\chi) \cdot H_2O. \qquad (2)$$

In the initial stage of experiment, many unstable colloid primary crystals of titania would be formed, which could act as nucleus, and further grow and aggregate to form bigger spherical particles having
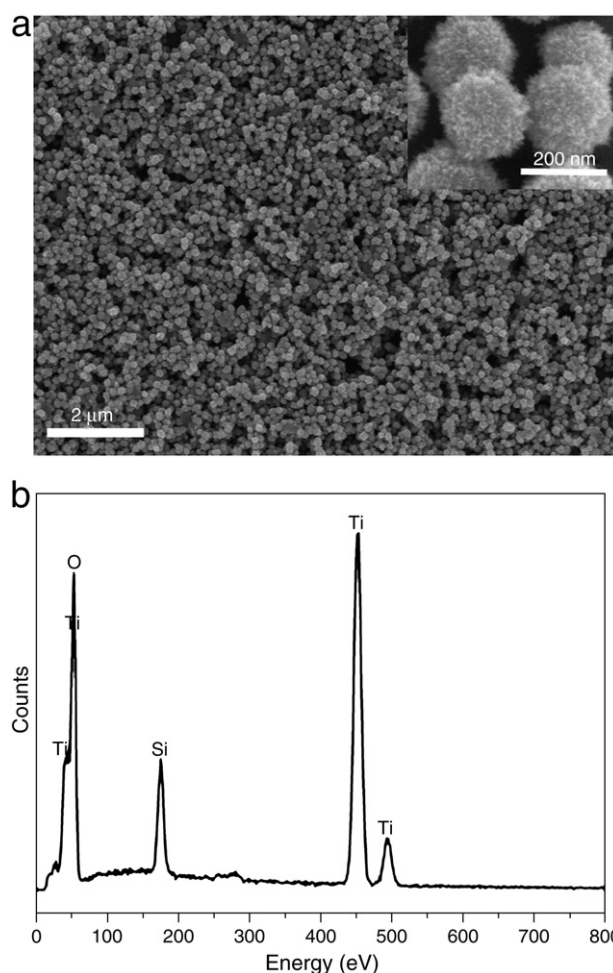

Fig. 1. (a) FESEM image of the spherical mesoporous titania (the inset is a magnification of the particles); and (b) EDX spectrum of the spherical mesoporous titania.

porous nature [24]. Fig. 1a shows the FESEM image of the as-synthesized sample. It can be seen that the size of spherical sample was comparatively uniformly sized. The diameter of the single dispersed spherical particle was about 200 nm and the surface of particles consisted of needle things. The EDX in Fig. 1b confirms the elemental composition of titanium and oxygen, silicon originated from the silicon substrate. The TEM images in Fig. 2a demonstrate that the precipitation in the solution was spherical titania particle with needle things, which agrees well to the FESEM examination. The HRTEM image of the as-synthesized mesoporous sample (Fig. 2b) shows that the crystal phase has already formed in the mesoporous particles. After calcinations at 300 °C and 500 °C, the samples have particle size in the range of 100–150 nm. The inserted patterns in Fig. 2c and e show the more detail microstructure of the nanoparticles. For the particles calcined at 300 and 500 °C, obvious mesoporous structure without long range order can be clearly observed in these patterns. The HRTEM images (Fig. 2d and f) indicate that the crystallinity of in the mesoporous particles increased with the increase of the temperature. The Fig. 3 displays the low-, high-resolution TEM and selected area electron diffraction images of the as-synthesized particles. Based on HRTEM observation, we found the obvious lattice planes in the surface of the needle. Meanwhile, the electron diffraction shown in the inset of Fig. 3 supported that the as-synthesized particles was crystalline TiO_2 at the outer layer.

Fig. 4 shows the FT-IR spectrum pattern of the spherical particles under different conditions in the range of 500–4000 cm^{-1}. The broad peaks at about 1640 cm^{-1} and 3420 cm^{-1} correspond to O–H groups and show the presence of water of hydration in the samples [24,25].
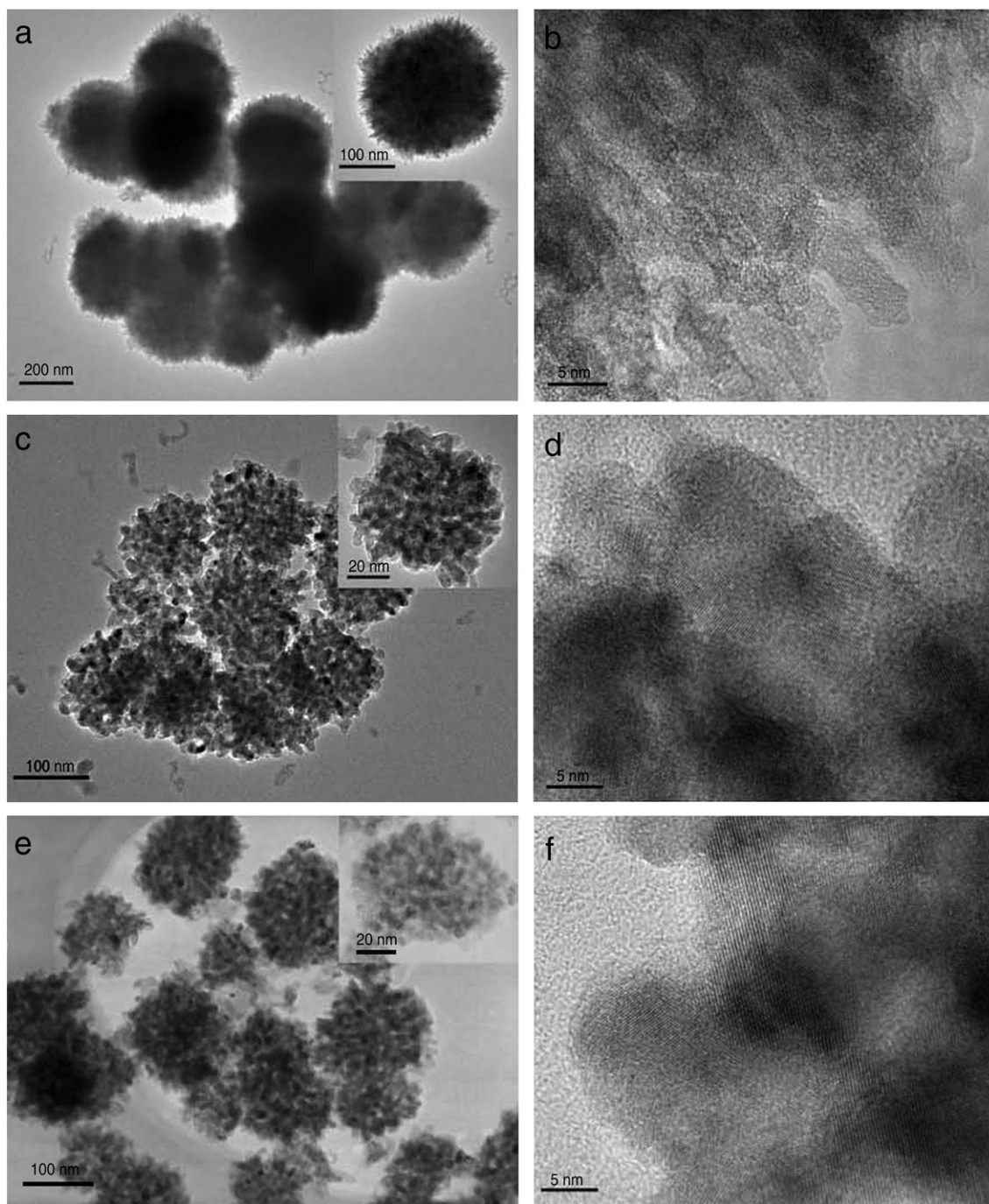
Fig. 2. TEM and HRTEM images of the spherical mesoporous titania: (a)–(b) as-synthesized mesoporous titania; (c)–(d) 300 °C for 2 h; (e)–(f) 500 °C for 2 h. The insets in (a), (c) and (e) are higher-magnification images of these particles under different conditions.

The peak at about 2970 cm^{-1} is normally attributed to symmetric and asymmetric stretching of –CH$_2$– groups and terminal CH$_3$– groups [26]. The weak peak around 1050 cm^{-1} is probably due to the N–C bond of triethanolamine [27]. It can be seen that all the peaks gradually get weak or even extinguish with the temperature increasing. Therefore, the water, alkoxyl group and triethanolamine are effectively reduced under the heat treatment. The content of residual triethanolamine is so little that it is difficult to find at 300 °C.

Brunauer–Emmett–Teller (BET) surface areas and Barret–Joyner–Halenda (BJH) pore size distributions of the as-synthesized and calcined samples are shown in Fig. 5. The isotherms exhibit the typical type IV, characteristic of mesoporous materials according to the IUPAC classification (Fig. 5a) [28]. The as-prepared sample showed a larger surface area of 198 m^2/g. While the sample was calcined at 300 and 500 °C for 3 h, it still presented a high specific surface area of 136 and 95 m^2/g, respectively. The pore size distribution curves indicate that the sample exhibit maxima at 3.82, 5.74 and 8.92 nm for the dried sample, 300 °C and 500 °C calcined samples, respectively (Fig. 5b). The variation of the pore size followed the inverse trend of the surface area with the calcination temperature. With the increase of calcination temperature, the surface area becomes small, and the pore size becomes larger. These are due to the crystallite growth and the collapse of the narrowest pores [29,30].

Furthermore, the effects of other experimental parameters were also investigated including concentration of Ti^{4+} ions, H$_2$O/n-butanol ratio (ω), and reaction temperature, as discussed in the following
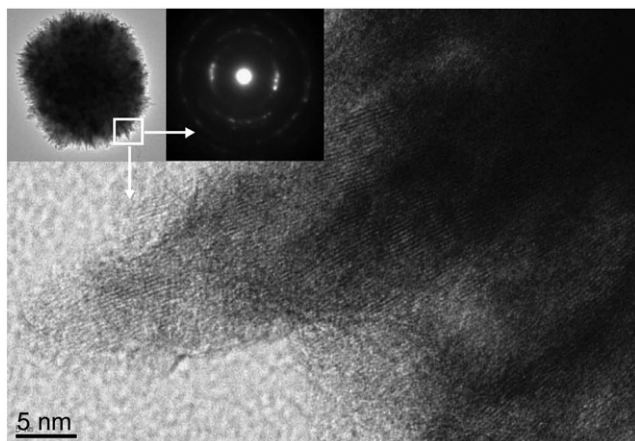
Fig. 3. TEM, HRTEM and SAED images of the spherical mesoporous titania.

context. However, more work needs to be performed to clarify the effects of these parameters on the surface areas and pore sizes.

The hydrolysis of Ti^{4+} ions is closely related to the concentration of Ti^{4+} ions. Here the effect of the concentration of Ti^{4+} ions on particle growth and the formation of crystal was further investigated. Fig. 6 shows the TEM images of the particles obtained at different concentration of Ti^{4+} values. At $[Ti^{4+}] = 0.25$ M, the obtained titania is irregularly arranged short rod-like by the aggregation of many titania spherical primary particle (Fig. 6a). When the concentration value was increased to 0.5 M, the porous titania nanosponges were observed (Fig. 6b). Further increasing the concentration value to 1 M, titania aggregates were formed. The titania aggregates are composed of hundreds of many nanofibers with a length of about 300 nm (Fig. 6c). At $[Ti^{4+}] = 2.5$ M, small colloids formed but they are difficult to clearly distinguish in shape and size as shown in Fig. 6d. According to the previous studies [31], there were $TiOH^{3+}$ ions in the $TiCl_4$ solution. When the concentration of Ti^{4+} ions was low, few $TiOH^{3+}$ ions adsorbed the TiO_2 nucleus, and the crystal growth habit was mainly affected by the interior rather than the exterior conditions. So these TiO_2 nucleuses grew along the [001] direction and formed the needle-like particles, and then these TiO_2 needle-like particles aggregated to form bigger spherical particles having porous nature under vigorous stirring. When the concentration of Ti^{4+} ions was very high, the plentiful HCl in the reaction process reduced the hydrolysis rate; the high concentration of H^+ increased the repulsive force among the colloids and restrained the growth of the particles.
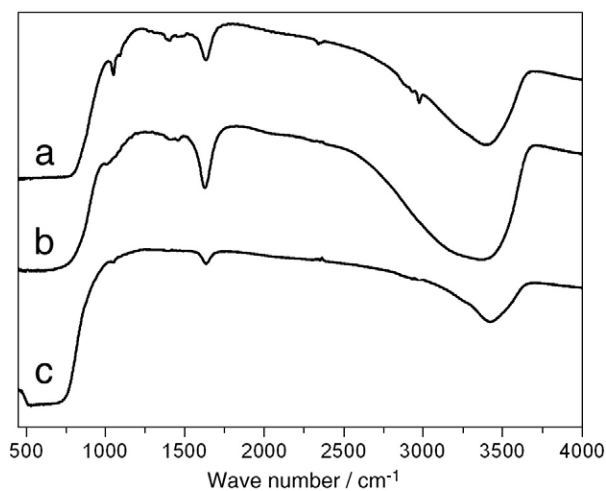

Fig. 4. IR of the mesoporous titania at different calcination temperatures (a) as-synthesized titania; (b) 300 °C for 2 h; (c) 500 °C for 2 h.
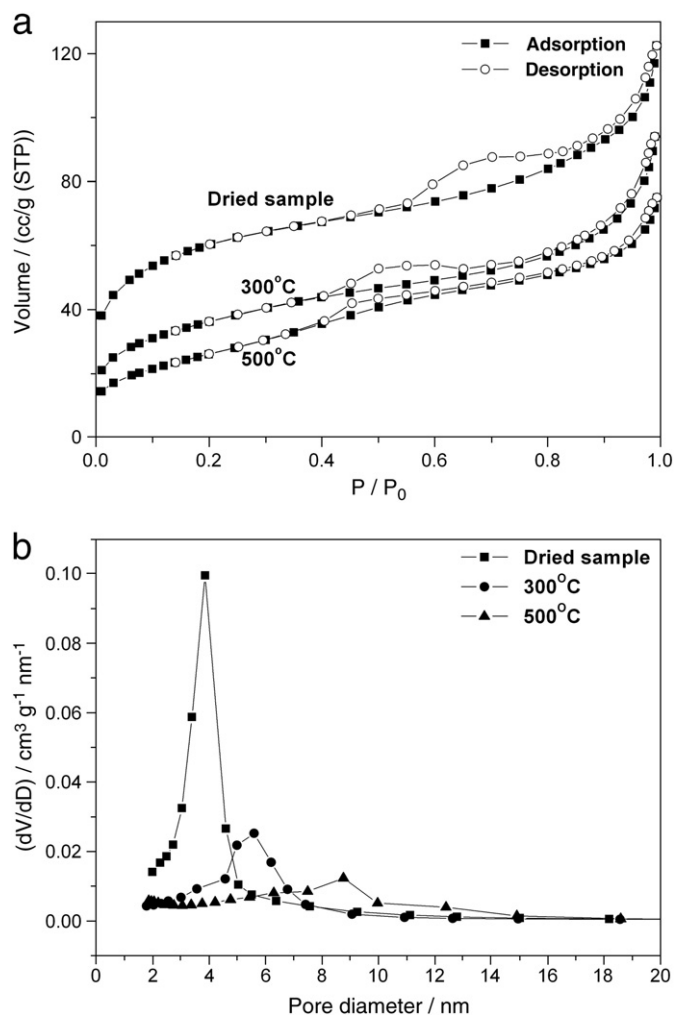

Fig. 5. (a) N_2 adsorption–desorption isotherm and (b) BJH pore size distribution plots of samples at different heated treatment temperatures.

XRD patterns of titania samples prepared at various concentration of Ti^{4+} ions are shown in Fig. 7. It was noted that every sample has rutile phase (Fig. 7a). However, broad and distinct peaks of anatase at 25.4, 48.1 ° appeared at $[Ti^{4+}] = 0.5$ M. Many XRD peaks of anatase may be overlapped with the peaks of rutile due to the faint intensity of the peaks. In order to identify the crystalline phase of the precipitate, these samples were treated at 300 °C for 2 h. As can be seen from Fig. 7b, when $[Ti^{4+}]$ was increased to ≥ 1 M, pure rutile phase was formed, which indicated that the concentration of Ti^{4+} ions in the solution is an important factor for the phase of the products. The previous works revealed that both anatase and rutile titania can grow from TiO_6 octahedra, and the phase transition proceeds by the rearrangement of these octahedral [32–34]. In high concentration of Ti^{4+}, the TiO_6 octahedra link each other in the straight chains by sharing equatorial edges, and then grow to rutile crystallites. In addition, a high concentration of HCl in the solution is in favor of the formation of rutile phase [35,36]. The concentration of HCl increases with the increase of concentration of Ti^{4+} ions in our work. It is beneficial to the formation of rutile type nucleus.

The XRD patterns in Fig. 8 show the effect of the water to n-butanol volume ratio on the phase of TiO_2 particles. During the preparation process, the reaction temperature and the concentration of Ti^{4+} ions were kept constant. It was noted that these as-synthesized titania were mixed phase in various water to n-butanol volume ratio (Fig. 8a), which suggested that the water to n-butanol ratio had no effect on the formation of phase in this process. When these samples
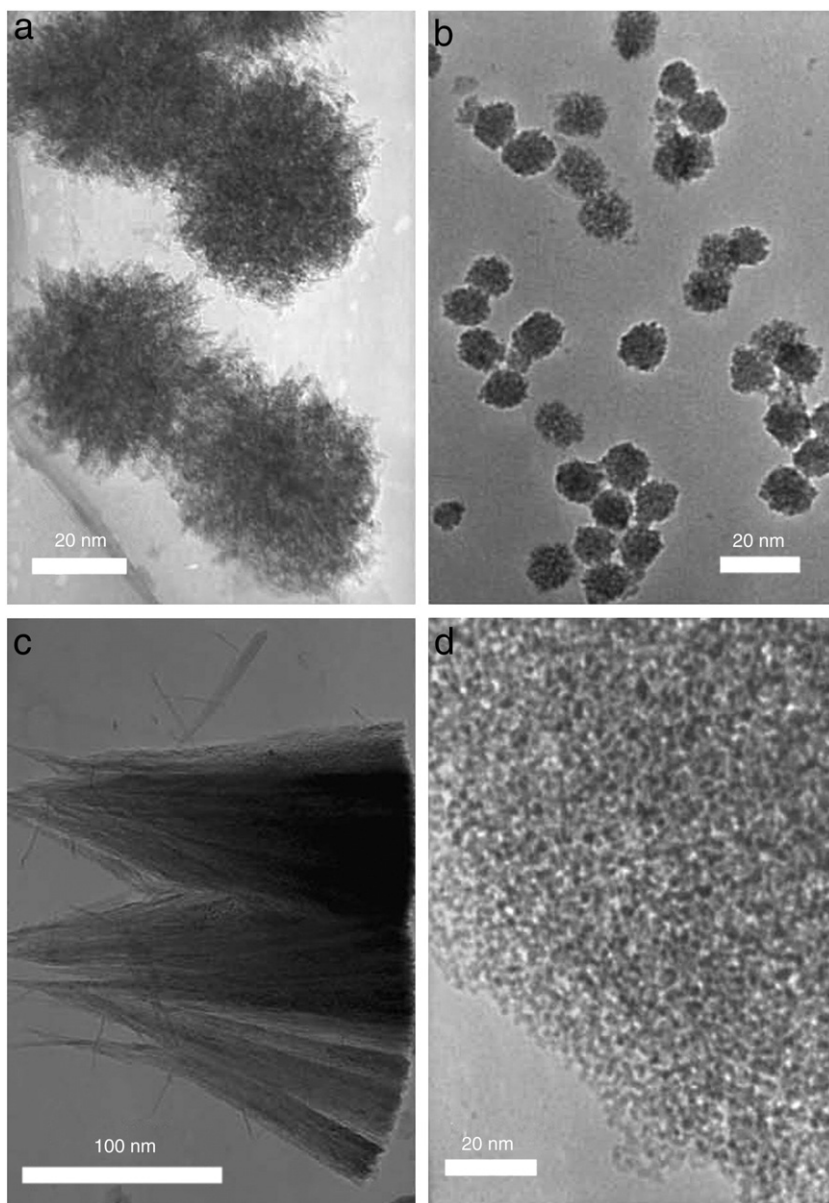
Fig. 6. Effect of the concentration Ti^{4+} ions on the shape of titania particles: (a) 0.25 M; (b) 0.5 M; (c) 1 M; (d) 2.5 M.

were calcined at 300 °C for 2 h, the XRD peaks of anatase and rutile were observed (Fig. 8b). These results further indicated that these as-synthesized samples were mixed phase. Fig. 9 presents the FESEM images of the samples prepared at different volume ratio of water to n-butanol. From Fig. 9, the needle-like things disappeared with the increase of the content of water (Fig. 7a and b). At the volume ratio values was 1/2, the spherical primary particles aggregated into larger particles. Further increasing the content of water, the precipitated particles are found to be very fine and the aggregations become intense (Fig. 9c and d). A possible reason for this may be that increasing the content of water is accompanied by an acceleration of the [Ti^{4+}] hydrolysis process and the dielectric constants of mixed solvents is increased [23].

Fig. 10 gives the FESEM images of the precipitates prepared at different temperatures. It is obvious that the irregular needle-like aggregates are obtained at 25 °C (Fig. 10a). When heated at 50 °C, some big particles are formed with diameter of 300–500 nm, along with some small ones (Fig. 10b). When heated at 80 °C, the precipitates are composed of small and discrete particles, the particle size is in the range of 200–300 nm (Fig. 10c). These results revealed that the optimum reaction temperature was about 80 °C. Fig. 11(a)–(c) shows the DLS

results of the samples prepared with various temperatures. The results show that the particle size of titania prepared at 80 °C has the smallest size than those prepared at 25 °C and 50 °C. The titania particles prepared at 25 °C (80–900 nm) and 50 °C (100 nm–1 μm) have larger width distribution than those prepared at 80 °C (100–400 nm).

4. Conclusions

We have developed a facile hydrolysis method to synthesize spherical mesoporous TiO$_2$ particles under mild conditions using titanium tetrachloride. The mesoporous particles were characterized with crystalline structure and had a certain thermal stability in the range of 300–500 °C. The specific surface area of the mesoporous TiO$_2$ calcined at 300 °C exceeded 136 m^2/g, and that of the samples after calcinations at 500 °C still have 95 m^2/g. The optimized experimental parameters for synthesis of such mesoporous particles are summarized as follows: titanium tetrachloride salt as a precursor with concentration of 0.25–0.5 M, reaction time being over 2 h by heating at about 80 °C. This method is very simple and easy to control or expand.
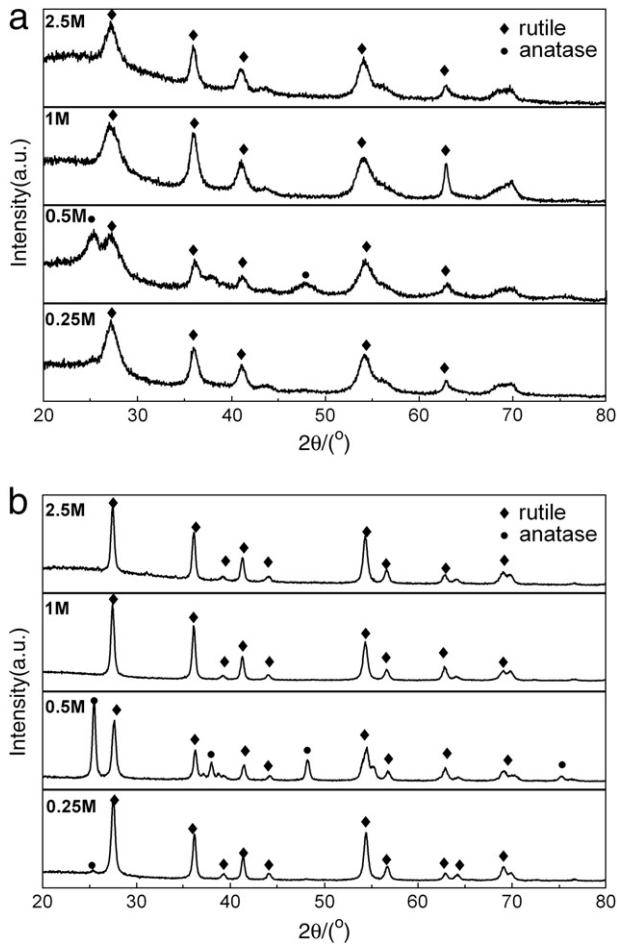
Fig. 7. (a) XRD patterns of as-synthesized titania under various concentration Ti^{4+} ions; (b) XRD patterns of these as-synthesized titania calcined at 300 °C for 2 h.
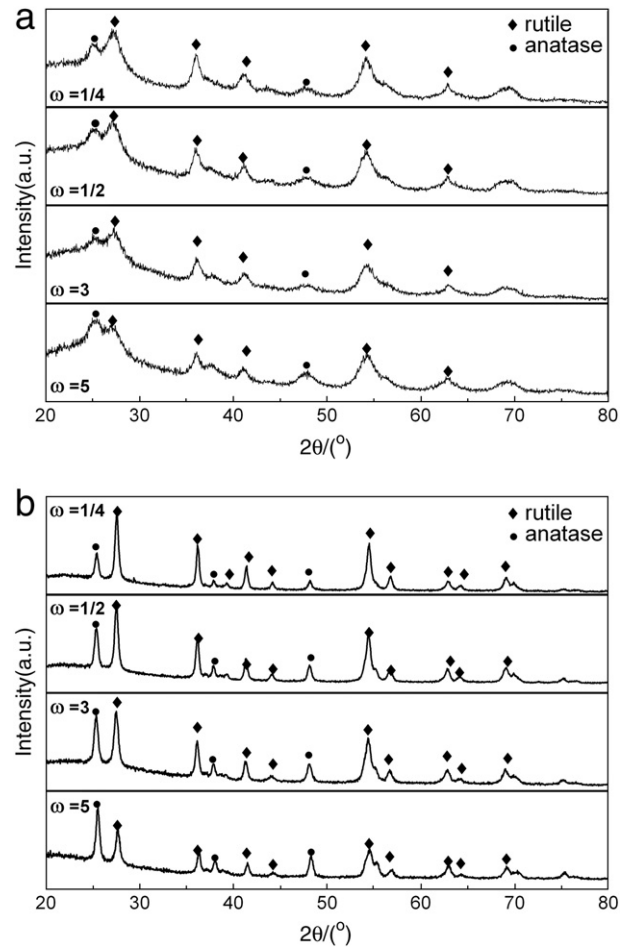
Fig. 8. (a) XRD patterns of as-synthesized titania under various volume ratio of H_2O/n-butanol (ω); (b) XRD patterns of these as-synthesized titania calcined at 300 °C for 2 h.
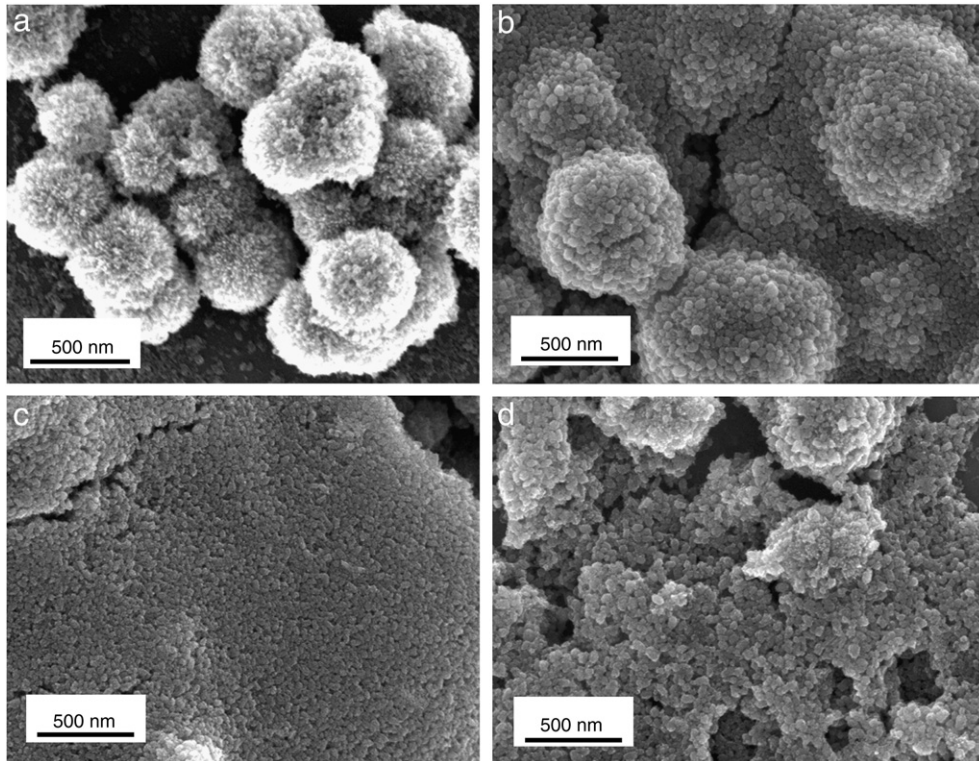

Fig. 9. FESEM images of as-synthesized samples under the reported volume ratio of H_2O/n-butanol (a) 1:4; (b) 1:2; (c) 3:1; (d) 5:1.
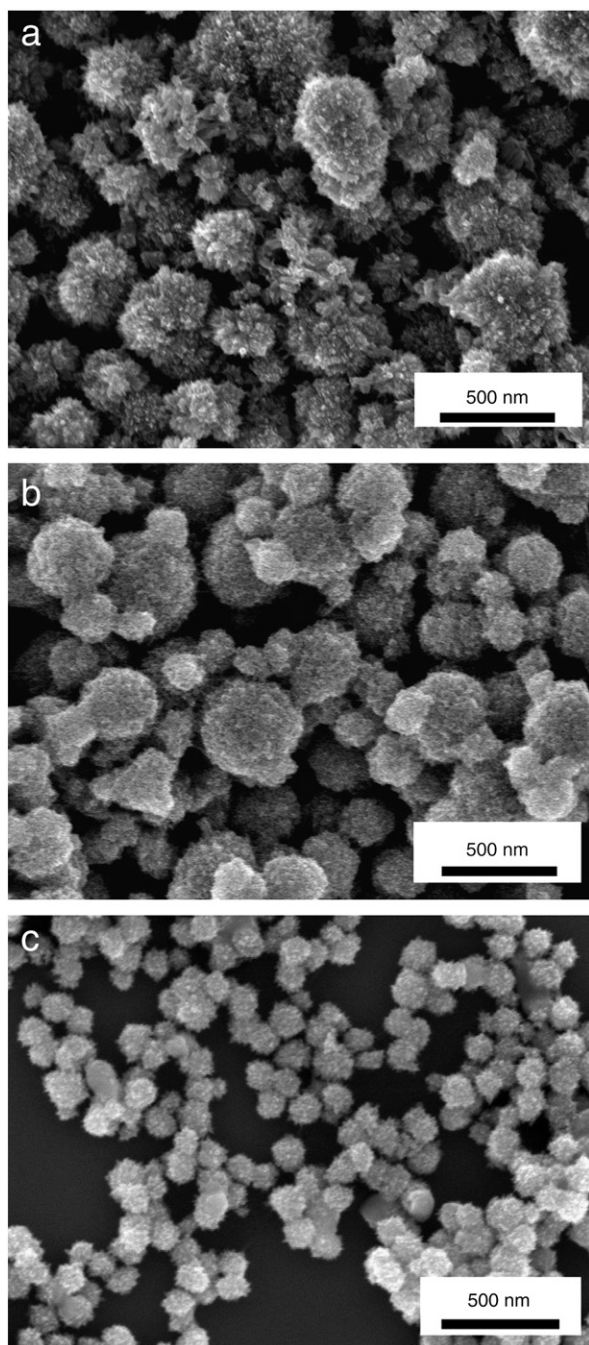
Fig. 10. Temperature dependence of titania particles formed (a) at 25 °C; (b) at 50 °C; (c) at 80 °C.

Fig. 11. Particles size distribution of titania (a) at 25 °C; (b) at 50 °C; (c) at 80 °C.

References

[1] D.Y. Wang, R.A. Caruso, F. Caruso, Synthesis of macroporous titania and inorganic composite materials from coated colloidal spheres—a novel route to tune pore morphology, Chem. Mater. 13 (2001) 364–371.
[2] H. Yoshitake, T. Tatsumi, Vanadium oxide incorporated into mesoporous titania with a BET surface area above 1000 m^2·g^{-1}: preparation, spectroscopic characterization, and catalytic oxidation, Chem. Mater. 15 (2003) 1695–1702.
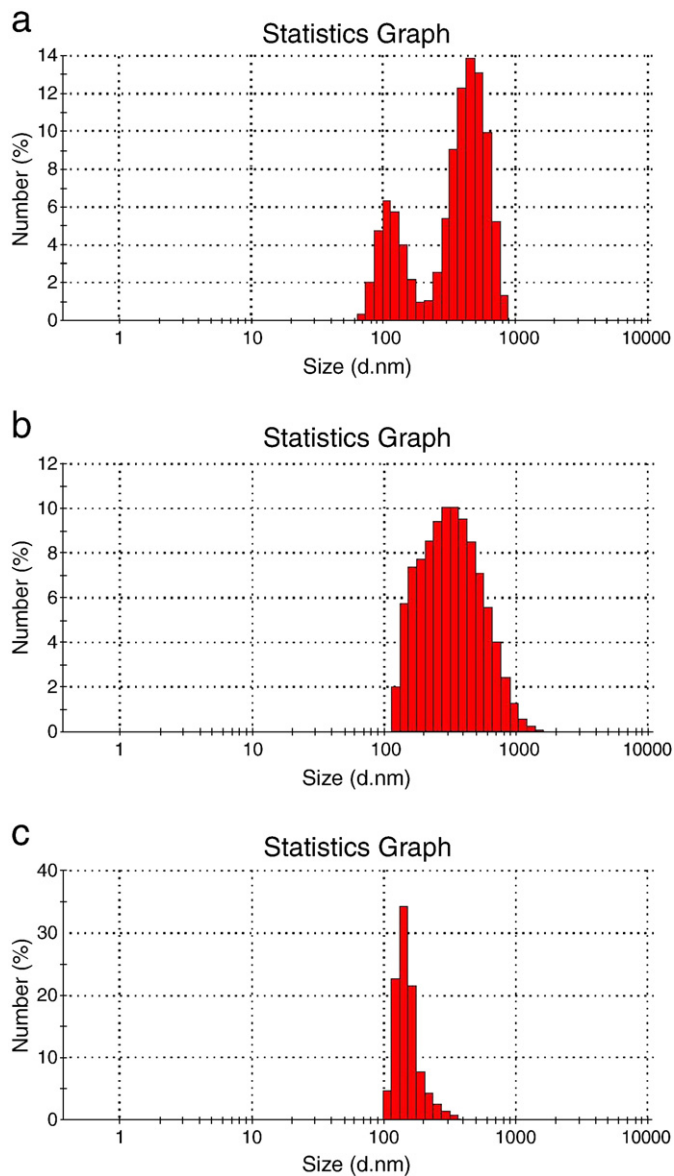[3] H. Li, Z. Bian, J. Zhu, Y. Huo, H. Li, Y. Lu, Mesoporous Au/TiO$_2$ nanocomposites with enhanced photocatalytic activity, J. Am. Chem. Soc. 129 (2007) 4538–4539.
[4] Z.H. Wang, T.S. Jiang, Y.M. Du, K.M. Chen, H.B. Yin, Synthesis of mesoporous titania and the photocatalytic activity for decomposition of methyl orange, Mater. Lett. 60 (2006) 2493–2496.
[5] D. Khushalani, G.A. Ozin, A. Kuperman, Glycometallate surfactants Part 2: Non-aqueous synthesis of mesoporous titanium, zirconium and niobium oxides, J. Mater. Chem. 9 (1999) 1491–1500.
[6] J.G. Yu, L.J. Zhang, B.Y. Cheng, R. Su, Hydrothermal preparation and photocatalytic activity of hierarchically sponge-like macro-/mesoporous titania, J. Phys. Chem. C 111 (2007) 10582–10589.
[7] D. Khushalani, G.A. Ozin, A. Kuperman, Glycometallate surfactants. Part 1: Non-aqueous synthesis of mesoporous silica, J. Mater. Chem. 9 (1999) 1483–1489.
[8] S. Fujihara, T. Maeda, H. Ohgi, E. Hosono, H. Imai, S.H. Kim, Hydrothermal routes to prepare nanocrystalline mesoporous SnO$_2$ having high thermal stability, Langmuir 20 (2004) 6476–6481.
[9] K.L. Frindell, J. Tang, J.H. Harreld, G.D. Stucky, Enhanced mesostructural order and changes to optical and electrochemical properties induced by the addition of cerium(III) to mesoporous titania thin films, Chem. Mater. 16 (2004) 3524–3532.
[10] D.W. Lee, S.J. Park, S.K. Ihm, K.H. Lee, One-pot synthesis of Pt-nanoparticle-embedded mesoporous titania/silica and its remarkable thermal stability, J. Phys. Chem. C 111 (2007) 7634–7638.
[11] B. Chi, L. Zhao, T. Jin, One-step template-free route for synthesis of mesoporous N-doped titania spheres, J. Phys. Chem. C 111 (2007) 6189–6193.
[12] D.M. Antonelli, J.Y. Ying, Synthesis of hexagonally packed mesoporous TiO$_2$ by a modified sol–gel method, Angew. Chem. Int. Ed. Engl. 34 (1995) 2014–2017.
[13] D.M. Antonelli, Synthesis of phosphorus-free mesoporous titania via templating with amine surfactants, Microporous Mesoporous Mater. 30 (1999) 315–319.

[14] Y. Yue, Z. Gao, Synthesis of mesoporous TiO$_2$ with a crystalline framework, Chem. Commun. (2000) 1755–1756.
[15] R. Yang, H. Yu, M. Li, Mesoporous properties of nanosized anatase titania powders prepared by urea hydrolysis with PEG dispersant, J. Mater. Sci. Lett. 22 (2003) 1131–1135.
[16] S. Cabrera, J.E. Haskouri, A. Beltrán-Porter, D. Beltrán-Porter, M.D. Marcos, P. Amorós, Enhanced surface area in thermally stable pure mesoporous TiO$_2$, Solid State Sci. 2 (2000) 513–518.
[17] K.M.S. Khalil, M.I. Zaki, Preparation and characterization of sol–gel derived mesoporous titania spheroids, Powder Technol. 120 (2001) 256–263.
[18] H.W. Wang, C.H. Kuo, H.C. Lin, I.T. Kuo, C.F. Cheng, Rapid formation of active mesoporous TiO$_2$ photocatalysts via micelle in a microwave hydrothermal process, J. Am. Ceram. Soc. 89 (2006) 3388–3392.
[19] H. Chen, K. Dai, T.Y. Peng, H.P. Yang, D. Zhao, Synthesis of thermally stable mesoporous titania nanoparticles via amine surfactant-mediated templating method, Mater. Chem. Phys. 96 (2006) 176–181.
[20] S. Karvinen, R.J. Lamminmäki, Preparation and characterization of mesoporous visible-light-active anatase, Solid State Sci. 5 (2003) 1159–1166.
[21] J.R. Xiao, T.Y. Peng, R. Li, Z.H. Peng, C.H. Yan, Preparation, phase transformation and photocatalytic activities of cerium-doped mesoporous titania nanoparticles, J. Solid State Chem. 179 (2006) 1161–1170.
[22] M. Inagaki, Y. Nakazawa, M. Hirano, Y. Kobayashi, M. Toyada, Preparation of stable anatase-type TiO$_2$ and its photocatalytic performance, Int. J. Inorg. Mater. 3 (2001) 809–811.
[23] H.K. Park, D.K. Kim, C.H. Kim, Effect of solvent on titania particle formation and morphology in thermal hydrolysis of TiCl4, J. Am. Ceram. Soc. 80 (1997) 743–749.
[24] S.B. Deshpande, H.S. Potdar, Y.B. Khollam, K.R. Patil, R. Pasricha, N.E. Jacob, Room temperature synthesis of mesoporous aggregates of anatase TiO$_2$ nanoparticles, Mater. Chem. Phys. 97 (2006) 207–212.
[25] M.S. Mohajerani, M. Mazloumi, A. Lak, A. Kajbafvala, S. Zanganeh, S.K. Sadrnezhaad, Self-assembled zinc oxide nanostructures via a rapid microwave-assisted route, J. Cryst. Growth 310 (2008) 3621–3625.
[26] C.R.K. Rao, D.C. Trivedi, Biphasic synthesis of fatty acids stabilized silver nanoparticles: role of experimental conditions on particle size, Mater. Chem. Phys. 99 (2006) 354–360.
[27] G. Yu, X. Wang, L. Zhu, D. Xu, Q. Ren, G. Zhang, X. Liu, Z. Sun, H. Fan, Crystallization process and microstructure of sol–gel derived Pb$_{0.9}$La0.1Ti$_{0.875}$O$_3$ fine fibers with a novel heat-treatment process, Solid State Sci. 10 (2008) 859–863.
[28] Y.H. Zhang, A. Weidenkaff, A. Reller, Mesoporous structure and phase transition of nanocrystalline TiO$_2$, Mater. Lett. 54 (2002) 375–381.
[29] T.A. Ostomel, G.D. Stucky, Free-standing mesoporous titania films with anatase nanocrystallites synthesized at 80 °C, Chem. Commun. (2004) 1016–1017.
[30] L.R. Pizzio, Mesoporous titania: effect of thermal treatment on the texture and acidic properties, Mater. Lett. 59 (2005) 994–997.
[31] Y.Y. Li, J.P. Liu, Z.J. Jia, Morphological control and photodegradation behavior of rutile TiO$_2$ prepared by a low-temperature process, Mater. Lett. 60 (2006) 1753–1757.
[32] H.B. Yin, Y. Wada, T. Kitamura, et al., Hydrothermal synthesis of nanosized anatase and rutile TiO$_2$ using amorphous phase TiO$_2$, J. Mater. Chem. 11 (2001) 1694–1703.
[33] M. Gopal, W.J. Moberlychen, L.C. De Jonghe, Room temperature synthesis of crystalline metal oxides, J. Mater. Sci. 32 (1997) 6001–6008.
[34] Y.H. Zhang, E.W. Shi, Z.Z. Chen, W.J. Li, X.F. Hu, Influence of solution concentration on the hydrothermal preparation of titania crystallites, J. Mater. Chem. 11 (2001) 1547–1551.
[35] J.H. Lee, Y.S. Yang, Effect of HCl concentration and reaction time on the change in the crystalline state of TiO$_2$ prepared from aqueous TiCl$_4$ solution by precipitation, J. Eur. Ceram. Soc. 25 (2005) 3573–3578.
[36] J.H. Lee, Y.S. Yang, Effect of hydrolysis conditions on morphology and phase content in the crystalline TiO$_2$ nanoparticles synthesized from aqueous TiCl$_4$ solution by precipitation, Mater. Chem. Phys. 93 (2005) 237–242.